J. Phys. Res. Edu., Vol. 1, March 2024

Na_2O Doped Solid State Battery Electrolytes: Preparation and Electrical Characterization

Rakesh Ram and Sanjib Bhattacharya*

Composite Materials Research Laboratory, UGC-HRDC (Physics),

University of North Bengal, District: Darjeeling-734013, West Bengal India.

Present work explores the development of Na_2O doped electrolytes and their conduction behavior. Electrical transport behavior (mixed conduction) of as-developed electrolytes has been investigated with respect to frequency and temperature. A nature of flat conductivity in the lower frequency window may be caused due to diffusional motion of Na^+. It is also noted that the conductivity shows dispersion near the high frequency regime. Electrical conductivity has also been analyzed with respect to temperature to explore their thermally activated nature. A little bit of difference in trajectories of current-voltage characteristics in both directions should make sense for their applications in the sectors of battery-electrolytes.

I. INTRODUCTION

In recent days, the availability of lithium in the earth's crust is decreasing, which is leading the research for alternative ways [1–3]. As an alternative, sodium ion batteries (NIBs) [1–3] could be thought of. Owing to the abundant storage and low cost preparation techniques, sodium ion batteries serve best to replace lithium ion batteries [4–6]. Here, Na_2O doped glassy electrolytes have been developed which serves as the electrolyte for NIBs in terms of exhibiting certain important features such as in electrochemical stability, sensors etc. [4–6]. Na_2O doped glassy electrolytes in solid form, is preferred over liquid electrolyte due to their higher stability and ease of access, which may lead us to develop Na_2O doped solid electrolytes with higher conductivity at ambient temperatures [6]. Study of various characteristics of such system has been done such as AC conductivity [7, 8]. Hopping frequency and conduction trajectories of Na^+ may be computed from Almond-west formalism [7, 8] at a frequency ω

$$\sigma(\omega) = \sigma_{dc}\left[1 + \left(\frac{\omega}{\omega_H}\right)^n\right], \tag{1}$$

where, σ_{dc}, ω_H, and n are referred to as low frequency conductivity, hopping frequency of Na^+, and the power law exponent, respectively.

So, the present work has been executed for the useful effect of research and teaching community both in line with the following objectives:

(i) Easy development of Na_2O doped solid electrolytes at low cost

(ii) To improve their transport behavior at various temperatures

(iii) To establish a correlation between transport of ions migration process and the dielectric relaxation process

(iv) To study the conduction mechanisms with comparison with others' works

(v) To explore the hopping frequency and allied parameters for analyzing and checking the efficiency of as-prepared electrolytes to be used for NIBs

II. EXPERIMENTAL PROCEDURE

New electrolytes, $x$$Na_2O$-$(1-x)$(0.2ZnO-0.8CdO) with x = 0.1 and 0.2 were prepared using solid state reaction method from reagent grade chemicals, Na_2CO_3, ZnO, and CdO. The chemicals were mixed with proper stoichiometric ratio in an alumina crucible, which was placed in an electric furnace. The temperature of the furnace was varied from 100℃ to 1200℃. The mixture was kept over there for 1 hour. In this way of heat-treatment, the composite materials were formed. The pallets of thicknesses 1-2 mm were developed from the mixture. Graphite paste was painted on both sides of the pallets for making electrodes. Here, graphite paste was used instead of conventional silver paste or gold coating in order to avoid polarization effects near the interface. HIOKI (model no. 3532-50) made LCR meter was used to accumulate electrical measurements readings. Current-Voltage dataset of as-developed system was taken by a dedicated electrometer (Keithley make, model No. 6514/E). Various phases in the as-developed system were confirmed from X-ray diffraction (Panalytical) study.

III. RESULTS AND DISCUSSIONS

A. DC Conductivity

DC conductivity data were plotted with different concentrations of the sample along with the activation energy. These data were interpreted using Arrhenius [9] model

$$\sigma_{dc} = \sigma_0 \, e^{-E_0/k_B T}, \tag{2}$$

where σ_0, E_0, k_B, and T are referred to as the pre-exponential factor, activation energy related to σ_{dc}, Boltzmann constant, and the absolute temperature, respectively. The DC conductivity and related activation energy are presented with respect to composition in Figs. 1(a) and 1(b), respectively. Gradual decrement in

DC conductivity with composition is observed in Fig. 1(a), which may attribute for existence of numerous defects [10]. Such defects may result the presence of non-bridging oxygens [11, 12]. According to existing literature [1, 11, 12], bridging oxygen is expected to participate in covalent bonding, playing a crucial role in forming Na–O bonding [1, 11, 12]. Consequently, bridging oxygen emerges as a major role in the DC conductivity mechanism by facilitating the mobile nature of Na^+. Conversely, a part of oxygen ions does not take part in the network [1, 11, 12], and it is proposed that these oxygens contribute to non-bridging configurations. These oxygen atoms are believed to give rise to non-bridging oxygen through permanently broken oxygen bonds[1, 11, 12], as discussed in the literature. A few oxygen atoms are expected to form non-bridging nature of structures, which are mainly caused for the trapping centres/ defects [1]. Such defect states are expected to form the constraints of motion of Na^+, which may in turn, increase the activation energy related to DC conductivity [1, 11, 12].

The glassy system doped with Li_2O and Na_2O as evident from other's work [13], exhibits low value of DC conductivity up to $x = 0.2$ in comparison with current investigation. This may be due to difference in structure with B_2O_3 and P_2O_5 as formers, which may contribute more stable structure [13]. In contrast, present work involves a combination of CdO and ZnO as the network former. The role of CdO may trigger for the development of defects in the present system [14], whereas ZnO acts as a stabilizer [15]. So, CdO and ZnO ratio can be altered to improve their electrical properties [16]. Moreover, the activation energy (E_0) related to DC conductivity in our system is lower than reported in other studies. This lower E_0 value indicates the absence of specific defect states related to grain boundaries, which typically result in a higher potential barrier [16]. In our context, "particular defect states" refer to defects that may arise from the charged states (D^+ and D^-) due to the existence of dangling-bond [1]. Absence of these defect states in the higher potential barrier window, as evidenced by smaller E_0 values, suggests the exemption of mutually connected polaronic conduction (bi-polaron) via Coulombic interaction [1]. The lack of grain boundaries is further supported by the absence of additional arcs in Fig. 1(a) may confirm a much higher DC conductivity in our system compared to the Na_2O-Li_2O system. This finding underscores the potential suitability of our system as an electrolyte for upcoming materials for the batteries.

B. Study of Alternating Current Conductivity

At different temperatures the conductivity spectra have been scrutinized, and such a curve for $x = 0.2$ is presented in Fig. 2(a). Examination of Fig. 2(a) reveals that AC conductivity spectra exhibit both thermal activation and frequency dependence [17, 18]. In the lower frequency range, the spectra display flat isotherms, akin to the conduction related to DC part. Alteration in electrical conduction patterns initiates at the hop-

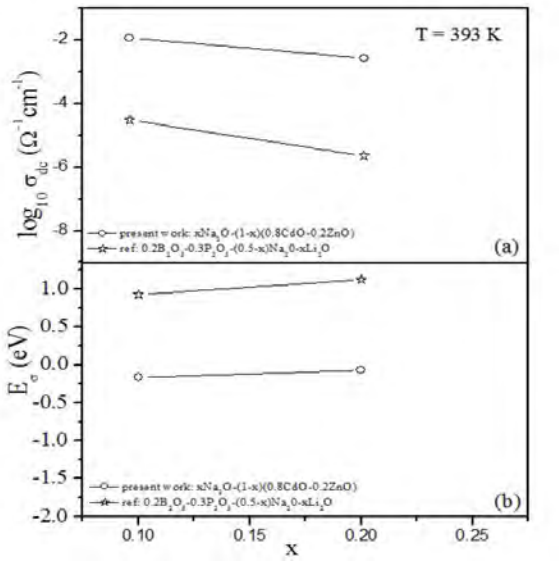

FIG. 1: (a) Comparison of DC conductivity with compositions with others' work. (b) Variation of activation energy corresponding to DC conductivity with compositions along with others work.

ping or leap frequency of charge-carriers [17], and after this frequency, distribution becomes evident. It was anticipated as the movement of charge-carriers are interrelated as well as confined within the high frequency range [19]. The Na_2O-doped system demonstrates a higher conductivity level of approximately 10^{-2} Ω^{-1} cm^{-1}, suggesting its potential as a promising electrolyte for next-generation battery materials. The thermal activation and frequency dependence observed in the AC conductivity spectra further emphasize the dynamic behavior of charge carriers.

Thermally excited character of AC conductivity has been examined at numerous frequencies to gain insights into the thermally activated nature of the present system at a specific frequency [18]. Figure 2(b) illustrates one such plot for $x = 0.2$ across different frequencies. The plot indicates a broad dispersion of AC conductivity in the vicinity of low-temperature window. Interestingly, as the temperature advances, the conductivity spectra are found to converge and collapse. It's worth noting that as the frequency rises, there is an accompanying increase in AC conductivity. This behavior underscores the dynamic relationship between temperature, frequency, and conductivity in the studied system, revealing its intricate thermally activated characteristics.

The data obtained in Fig. 2(a) were meticulously examined by Eq. (1), in order to acquire comprehensive insights for the conduction spectra which rely on frequency. A rigorous data best fitted graphs [19] using Eq. (1). The fitting process is undertaken with the goal of attaining a robust and accurate representation of the underlying relationship between the variables involved. The fitting process has yielded essential parameters, including the hopping frequency (ω_H), DC conductivity (σ_{dc}), and frequency exponent (n). The

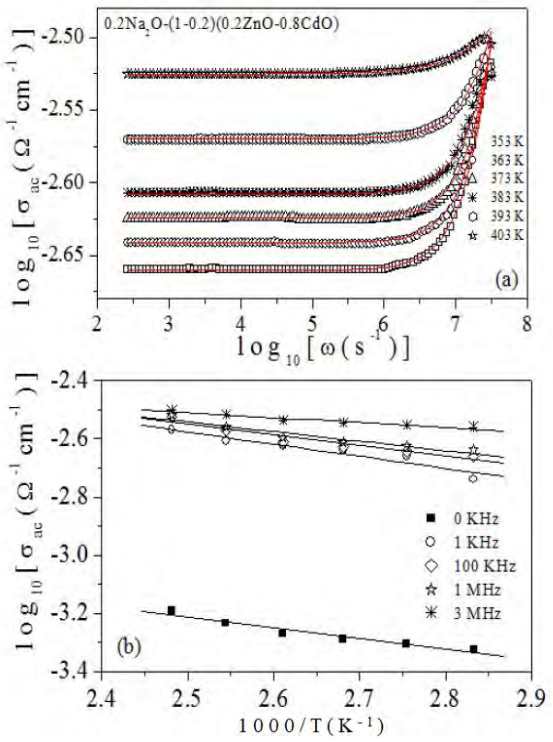

FIG. 2: (a) AC conductivity spectra for $x = 0.2$ at different temperatures. (b) Reciprocal temperature dependence of AC conductivity at different fixed frequencies for a particular composition.

estimation and interpretation of these fitting parameters contribute to a deeper understanding of the underlying mechanisms governing the conductivity in the studied system, facilitating meaningful comparisons and predictions. The estimated values of ω_H at 393 K and related activation energy have been presented in Fig. 3(a). The plot reveals a similar trend to that observed in DC conductivity.

The power law model [17], as outlined by Sidebottom, offers the parameter "n," which may be linked with the nature of transport trajectories in various dimensions [20]. Sidebottom's approach [21] reveals a value of n around 0.67, which signifies the Ag^+ tridimensional movement in MoIO4 (iodo-molybdate) glassy systems. This concept may showcase an independent event of temperature as well as concentration. A more in-depth investigation indicates that an average value of n around 2.72 can be regarded as a concept of fractal dimensionality [22].

Figure 3(b) presents the average values of n with respect to different compositions. This representation allows for a visual exploration of the dimensionality characteristics across the studied compositions. The observed trends in n provide valuable insights into the transport trajectories and the complex nature of motion of charge carriers within the system. Figure 3(b) shows that the value of n can be sometimes higher than 1 (for $x = 0.2$) and sometimes lower than 1 (for $x = 0.1$). With lower concentration of Na^2O the Na^+

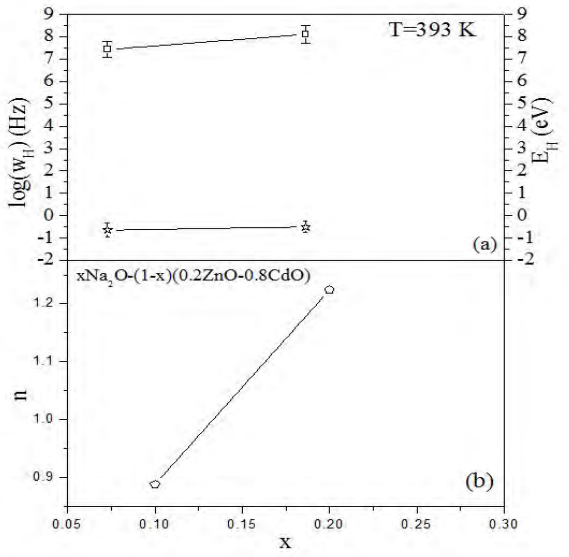

FIG. 3: (a) Hopping frequency vs concentration at a particular temperature T=393 K. (b) Frequency exponent(n) with compositions.

ion motion is dominated by electron or polaron. As the concentration of Na_2O increases the conduction is again dominated by Na+ ion motion over electron or polaron hopping.

The activation energy depicted in Figure 1(b) demonstrates an increase with increasing x, suggesting a potential shift in conduction mechanisms. This phenomenon could be attributed to the dynamics of Na^+ ions encountering a value of barrier potential. Another plausible explanation could involve the existence of an increasing number of oxygens that are not bridge oxygens for concentrations ranging from 0.10 to 0.2. This presence may prompt the release of more electrons from ZnO. The additional electrons from ZnO will be quickly liberated due to its presence, given the expectation that Na^+ is likely to form bonds with O^-. This line of reasoning leads to the consideration of hopping of small polarons as the major part of electrical conduction with lower Na_2O content.

Conversely, with an increase in Na^+, more bridging oxygens are supposed to be linked with Na^+ in terms of formation of Na^+-O^{-2}. Consequently, conductivity is anticipated causing domination due to dynamic behavior of Na^+ with increasing value of compositions. In summary, the magnitude of frequency exponent might be linked to the polaron-to-ion transferring mechanism as the quantity of Na_2O varies from lower to higher concentrations. The related activation energy is found to be crucial to overcome potential barrier associated with these conduction mechanisms. This discussion provides insights into the dynamic interplay between composition, conduction mechanisms, and activation energy in the studied system.

By manipulating the electric field, one can anticipate the thermal process for making the charge carriers active for electrical conduction in disordered solids [23, 24]. Jonscher's universal power law is often con-

sidered appropriate when employing it to analyze the AC conductivity data of amorphous semiconductors [23, 24]. It may be expressed as [23, 24]:

$$\sigma(\omega) = \sigma_0 + A\omega^S. \tag{3}$$

Here, σ_0, A and S are referred to as DC conductivity, coefficient and the power of frequency, respectively. To explore the character of AC conductivity in high frequency range, initiatives have been taken by many researchers [25–27]. AC conductivity data in the higher frequency window have been plotted in Fig. 4(a) for $x = 0.2$ at numerous temperatures, which illustrates a linear relationship as well as thermally activated nature. Eq. (3) is used to interpret the AC conductivity data in terms of best-fit method. Slopes of each best-fit line of the experimental data provide the values of S. It is inferred from the Fig. 4 that different conduction mechanisms with varying slopes, S may underlie the conductivities at low and high temperature at various frequency ranges [1].

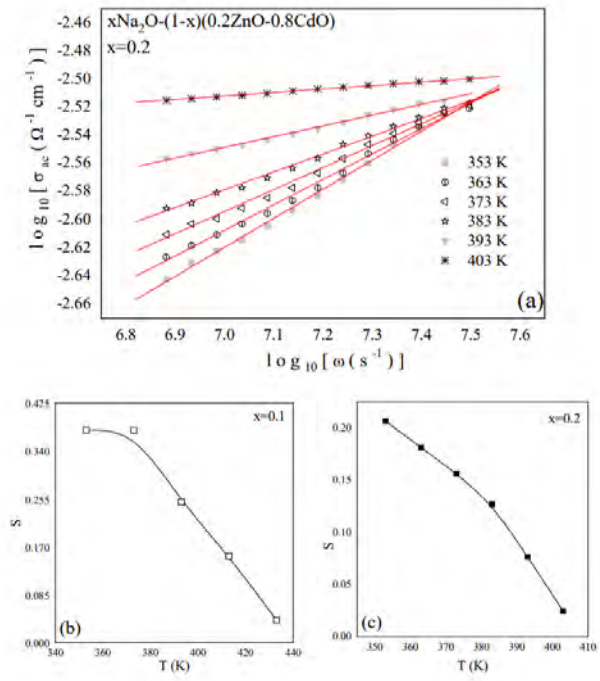

FIG. 4: (a) High conducitivity spectra for x=0.2 at various temperatures, solid straight lines indicates the best fitted straight line fits. (b) S-T plots for x=0.1 and (c) x=0.2.

The other samples prepared in the similar manner also exhibit a same type of AC conduction process within higher frequency regime. In the lower frequency region the VRH (variable range hopping) model [28–30] is applied for the probable conductivity process. Drawing from the defect model developed by Ingram *et al* [31], the characterization of the effectiveness of conductivity is accurately performed in the

high-temperature regions. The current researches [32] proposes in the lower frequency region that the polaron hopping aided by phonons is caused by the characteristic Ag–S vibration, whereas in the higher frequency regions it is caused by the unequal elongating vibrational modes of Zn–Te–Se bonding —forming primary portion of the conductivity process. Hence, it is common practice to figure out the concept of conduction behavior within higher frequencies in relation with wide temperature window.

Estimated values of S are plotted against absolute temperature in Fig. 4(b) and Fig. 4(c) for $x = 0.1$ and 0.2 respectively to explore their nature of conduction. Successful attempts have been made to establish such experimental findings in terms of fitting experimental data using most suitable correlated barrier hopping (CBH) model [26, 33, 34].

The CBH model [26, 33, 34] predicts the involvement of charge carriers (polarons) in terms of paired hopping process in as definite trajectory. In such process, a current transfer among localized sites near the Fermi level could be approximated. According to this model, the expression for S is given by [33]:

$$S = 1 - \frac{6k_BT}{W_m + k_B(T - T_0)\ln(\omega\tau_0)}. \tag{4}$$

Here, W_m is referred to the maximum barrier height, k_B is the Boltzmann constant, T is the absolute temperature, T_0 may be considered as the temperature for making S unity and τ_0 can be supposed to be the relaxation period. The bold curves in Fig. 4(b) and Fig. 4(c) represent the best-fit curves using Eq. (4).

For AC conductivity, the CBH model is given by

$$\sigma_{ac} = \frac{1}{24}n_0\pi^3 N(E_F)^2\varepsilon\varepsilon_0\omega R_{H\omega}^6. \tag{5}$$

Here, n_0 is referred to as the number of polarons participated in the hopping process, $N(E_F)$ represents the concentration of pair states, $R_{H\omega}$ means the hopping distance at frequency ω. At this moment, the bi-polar hopping mechanism is likely to consider primarily the main conduction process.

C. Current-Voltage Characteristics

To assess the suitability of the current system as a battery electrolyte, the researchers investigated the current–voltage characteristics of prepared samples. An example of such characteristics is presented in Fig. 5 for $x = 0.2$ in both the forward and backward directions. Figure 5 clearly shows the system under study displays a smooth straight curve having a consistent slope and there is no variation in back and forth ways. This observation clearly suggests Debye-like relaxation [18, 35–38] and dynamic resistance under a narrow range of applied voltage.

The content of ZnO within the system is used to stabilize the dynamic resistance distribution in this context as an impact of phonon vibration. Robert Hill and D.A. Dissado proposed that, the arrangement of

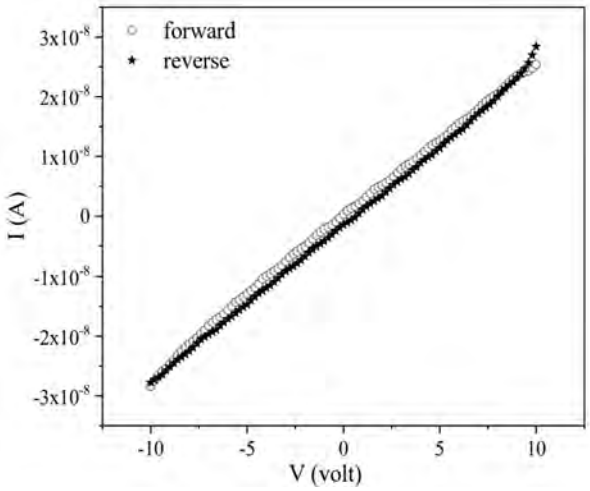

FIG. 5: I-V characteristics for $x = 0.2$.

relaxation time [18, 38] in the non-Debye process is linked to a δ-function value, indicating a highly rapid process. In contrast, δ-function value associated with a slow process characterized by a rapid decline in relaxation time indicates a Debye-like relaxation process. It is an indication of mixed type charge carriers stable conduction process as anticipated by the slower declination process of Debye-like relaxation mechanism. As observed from current-voltage characteristics in Figure 5 the nearly zero gap in the conduction paths in both the forward and backward direction the glass system doped with Na_2O is very much suitable as an electrolytes for upcoming era of batteries.

D. Relaxation process in the present system

The electrical relaxation characteristics of the investigated system were analyzed through the real (M') and imaginary (M'') components of electrical modulus framework [39], employing the following expressions:

$$M^*(\omega) = \frac{1}{\varepsilon^*(\omega)} = \frac{\varepsilon'(\omega)}{[\varepsilon'(\omega)]^2 + [\varepsilon''(\omega)]^2} + i\frac{\varepsilon''(\omega)}{[\varepsilon'(\omega)]^2 + [\varepsilon''(\omega)]^2} = M'(\omega) + iM''(\omega). \quad (6)$$

Figure 6(a) illustrates the graphical plot of imaginary component of electric modulus (M'') with respect to frequency for the samples $x = 0.1$ and $x = 0.2$ at a particular temperature (393 K). it is observed that M'' spectra exhibit a single relaxation peak where the height of the peak was increasing with higher value of x. The peak of the plots corresponds to the maximum value of frequency (ω_m) which is utilized to find the value of relaxation time (τ) from the relation $\tau = 1/\omega_m$.

Approximating the present relaxation process as Debye type, the relaxation time may be expressed as

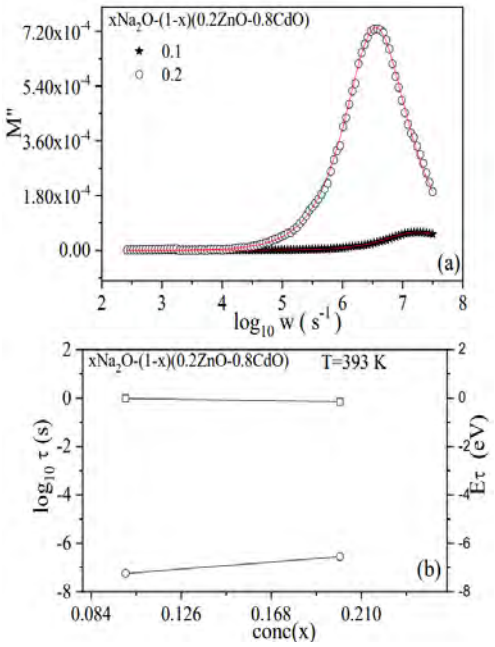

FIG. 6: (a) Modulus spectra for x=0.1 and x=0.2 (b) relaxation times and activation energy corresponding to relaxation times with compositions.

[18, 38]:

$$\tau = \tau_0 \, e^{-E_\tau / k_B T}. \tag{7}$$

Here, τ_0, k_B and T are referred to as the pre-exponential factor, Boltzmann constant and the absolute temperature, respectively. Equation (7) is used for least square fitting of the experimental data which yield relaxation times energy barrier E_τ. In Fig. 6(b), τ at a fixed temperature and their associated activation energies (E_τ) are presented. Notably, Fig. 6(b) shows that τ increases whereas E_τ decrease with varying compositions.

For compositions with lower Na_2O content, a short-time relaxation process is presumed, likely associated with the conduction of polarons. The overall relaxation mechanism within the current material under study is elucidated when it is associated with the lowest oscillations of sodium ions in compositions featuring higher quantity of Na_2O.Consideration is given to all types of lattice vibrations during relaxation mechanism for dielectrics.

The values of structural parameters (β) [37, 38] against composition is given in Table I. The nature of change of β values may also be employed to identify a definite transition from polaron hopping to ionic conduction [1].

x	$\beta(\pm 0.01)$
0.1	0.793
0.2	0.887

TABLE I: Structural parameters with compositions.

IV. CONCLUSION

Present study reveals the development and electrical characterization of glassy electrolytes, xNa$_2$O-$(1-x)$(0.2ZnO-0.8CdO) with $x = 0.1$ and 0.2 for possible applications for batteries. The analysis included the behavior of AC conductivity and relaxation process of as-developed system. The power law model yielded the frequency exponent (n), providing insights into the conduction trajectories in numerous dimensions. For x values of 0.20, the observed "n" values was occasionally higher than 1, indicating the potential presence of polaron-ion conductivity in the system. By the application of CBH-model the conductivity mechanism of electrons was recognized, elucidating the pathways of polarons hopping in pairs through the transfer of current among specific locations. Three-dimensional Na^+ motion was found out for samples with a higher Na_2O content. The present system demonstrated significantly greater direct current conduction process relative to Na_2O-Li_2O system, confirming the suitability of the present system as electrolytes for new-generation battery materials. The I–V characteristics exhibited a a little bit difference in displacement trajectories in both directions, suggesting it as a promising candidate for advanced battery electrolytes.

ACKNOWLEDGMENTS

Dr. Sanjib Bhattacharya thankfully acknowledge to Science and Engineering Research Board, Govt. of India via Sanction No. CRG/2023/000046 for financial assistance for the present study.

* Electronic address: ddirhrdc@nbu.ac.in

[1] B Karmakar, K. Rademann, and A. Stepanov, Glass nanocomposites: synthesis, properties and applications, Elsevier Publication, 2016.

[2] J. Y. Hwang, S. T. Myung, and Y. K. Sun, Chem. Soc. Rev., **46**, 3529 (2017).

[3] L. P. Wang, L. Yu, X. Wang, M. Srinivasan, Z. J. Xu, Journal of Materials Chemistry A, **3**, 9353 (2015).

[4] H. Aono, and Y. Sadaoka, Chemistry Letters, **29**, 34 (2000).

[5] I. A. Sokolov, V. N. Naraev, I. V. Murin, A. A.Pronkin, and A. V. Naraev. Russian journal of applied chemistry, **75**, 1240 (2002).

[6] Y. Zhao et al., Bulletin of Materials Science, **43**, 1 (2020).

[7] R. Cheruku, L. Vijayan, and G. Govindaraj, Materials Science and Engineering: B, **177**, 771 (2012).

[8] M. M. Ahmad, Physical Review B, **72**, 174303 (2005).

[9] L. K. Sudha, R. Sukumar, and K. Uma Rao, Int. J. Mater. Mech. Manuf. **2**, 96 (2014).

[10] E. D. Cubuk, S. S. Schoenholz, E. Kaxiras, and A. J. Liu, J. Phys. Chem. B **120**, 6139 (2016).

[11] F. A. Abdel-Wahab, A. M. Fayad, M. Abdel-Baki, and H. AbdelMaksoud, J. Non-Cryst. Solids **500**, 84 (2018).

[12] J. F. Stebbins and Z. Xu, Nature **390**, 60 (1997).

[13] J. S. Ashwajeet, T. Sankarappa, R. Ramanna, T. Sujatha, and A. M. Awasthi, AIP Conf. Proc. **1675**, 020017 (2015).

[14] A. Karmakar and A. Ghosh, J. Nanopart. Res. **13**, 2989 (2011).

[15] S. Bhattacharya and A. Ghosh, Appl. Phys. Lett. **88**, 133122 (2006).

[16] S. Shawuti, M. M. Can, M. A. Gulgun, S. Kaneko, and T. Endo, Compos. Part B: Eng. **147**, 252 (2018).

[17] S. Bag, P. Das, and B. Behera, J. Theor. Appl. Phys. **11**, 13 (2017).

[18] Y. B. Saddeek, A. A. El-Maaref, M. G. Moustafa, M. M. El-Okr, and A. A. Showahy, J. Mater. Sci.: Mater. Electron. **29**, 9994 (2018).

[19] V. V. Korotyeyev, V. A. Kochelap, V. V. Kaliuzhnyi, and A. E. Belyaev, Appl. Phys. Lett. **120**, 252103 (2022).

[20] M. Novy, H. Avila-Paredes, S. Kim, and S. Sen, J. Chem. Phys. **143**, 241104 (2015).

[21] D. L. Sidebottom, Phys. Rev. Lett. **83**, 983 (1999).

[22] L. Mancini, C. Janot, L. Loreto, R. Farinato, J. Gastaldi, and J. Baruchel, Philos. Mag. Lett. **78**, 159 (1998).

[23] C. Tsonos, Curr. Appl. Phys. **19**, 491 (2019).

[24] A. Dhahri, E. Dhahri, and E. K. Hlil, RSC Adv. **8**, 9103 (2018).

[25] D. Das and S. Samanta, ACS Appl. Electr. Mater. **3**, 1634 (2021).

[26] H. Bouaamlat, N. Hadi, N. Belghiti, H. Sadki, M. NaciriBennani, F. Abdi, M. Abarkan, T.-d. Lamcharfi, and M. Bouachrine, Adv. Mater. Sci. Eng. 2020, 1 (2020).

[27] A. Langar, N. Sdiri, H. Elhouichet, and M. Ferid, Results Phys. **7**, 1022 (2017).

[28] B. I. Shklovskii, A. L. Efros, B. I. Shklovskii, and A. L. Efros, Electronic Properties of Doped Semiconductors, **45**, 202 (1984).

[29] R. Plugaru, T. Sandu, and N. Plugaru, Results Phys. **2**, 190 (2012).

[30] N. T. T. Hong, V. S. Zakhvalinskii, T. T. Pham, N. T. Dang, E. A. Pilyuk, G. V. Rodriguez, and T. V. Vu, Mater. Res. Express **6**, 055915 (2019).

[31] B. J. Ingram, B. J. Harder, N. W. Hrabe, T. O. Mason, and K. R. Poeppelmeier, Chem. Mater. **16**, 5623 (2004).

[32] A. Chamuah, K. Bhattacharya, C. K. Ghosh, and S. Bhattacharya, Mater Today: Proc. **66**, 3218 (2022).

[33] Ajili, B. Louati, and K. Guidara, J. Mater. Sci.: Mater. Electron. **29**, 8649 (2018).

[34] M. Singh, K. L. Bhatia, N. Kishore, P. Singh, and R. S. Kundu, J. Non-Cryst. Sol. **180**, 251 (1995).

[35] F. Tian and Y. Ohki, IEEE Trans. Dielectrics Electr. Insul. **21**, 929 (2014).

[36] M. Rajnak, B. Dolnik, J. Kurimsky, R. Cimbala, P. Kopcansky, and M. Timko, J. Chem. Phys. **146**, 014704 (2017).

[37] C. R. Mariappan, G. Govindaraj, S. V. Rathan, and G. V. Prakash, Mater. Sci. Eng: B **123**, 63 (2005).

[38] J. Liu, C. G. Duan, W. G. Yin, W. N. Mei, R. W. Smith, and J. R. Hardy, J. Chem. Phys. **119**, 2812 (2003).

[39] S. N. Mohamed, M.K. Halimah, R. H. Y. Subban, A. K. Yahya, Physica B: Condensed Matter, **602**, 412480 (2021).